ELSEVIER

Journal of Alloys and Compounds 227 (1995) 157–166

Journal of ALLOYS AND COMPOUNDS

Influence of the nature of milling media on phase transformations induced by grinding in some oxides

S. Begin-Colin[a], G. Le Caër[a], M. Zandona[a], E. Bouzy[b], B. Malaman[c]

[a]*Laboratoire de Sciences et Génie des Matériaux Métalliques, CNRS URA 159, Ecole des Mines, F-54042 Nancy Cedex, France*
[b]*Laboratoire de Métallurgie des Matériaux Polycristallins, ISGMP, Université de Metz, Ile du Saulcy, F-57045 Metz Cedex 01, France*
[c]*Laboratoire de Chimie du Solide Minéral, CNRS URA 158, Université de Nancy I, BP239, F-54506 Vandoeuvre-Les-Nancy Cedex, France*

Received 20 September 1994; in final form 2 February 1995

Abstract

Polymorphic transformations induced by dry ball milling in an argon atmosphere have been investigated in various oxides (TiO_2, SnO_2, Y_2O_3, WO_3) by X-ray diffraction, Mössbauer spectroscopy and transmission electron microscopy (TEM). The transformations have been found to depend on the nature of the milling media, particularly when reduction reactions take place between grinding tools and oxide particles. When ground with steel tools, cubic yttria is transformed into a monoclinic modification as reported in the literature, while tin oxide is reduced. When ground with zirconia tools, cubic yttria with a bixbyite type structure is transformed into cubic yttria with a fluorite type structure, while monoclinic tungsten oxide is transformed into a cubic oxide with an ReO_3 type structure. Plausible structural explanations are proposed. In all cases, nanometre-sized domains have been observed by TEM even after grinding times as short as some minutes.

Keywords: Grinding; Oxides; Polymorphic transformations; Milling media

1. Introduction

Polymorphic transformations take place during dry milling in various oxides [1]. Various polymorphs may appear transiently even for very short milling times [2]. Many oxides formed in such conditions are metastable at ambient temperature and pressure and exist in equilibrium only at high temperature and/or at high pressure. Some recent articles report for instance on: (1) the transformation of transition aluminas (γ, κ, χ) into α alumina [3,4]; (2) the transient formation of a high-pressure modification of TiO_2 (TiO_2-II with an α-PbO_2-type structure) after some minutes of grinding of anatase [5], whether milling is performed with zirconia or with steel grinding tools [2]; (3) the development of a high-temperature–high-pressure monoclinic modification of Y_2O_3 by grinding of cubic Y_2O_3 with steel vial and balls [5], when almost complete amorphization of Y_2O_3 occurs during prolonged grinding [6]; and (4) the transient formation of an amorphous Nb_2O_5 oxide during the transformation process of the monoclinic H–Nb_2O_5 phase into a pseudo-hexagonal modification [7,8].

Such polymorphic transformations not only depend on the dynamical conditions of grinding [9–11], but may also depend on the nature (metals, oxides) of the grinding tools [12,13]. Stoichiometry changes may, for instance, be induced by a reduction reaction at the interface between oxide particles and metallic balls. We have therefore investigated the influence of the nature of grinding media on the polymorphic transformations induced by grinding in some oxides (SnO_2, Y_2O_3, WO_3). Particles of yttria are conveniently dispersed in alloys by mechanical alloying, as first shown by Benjamin [14]. Orthorhombic WO_3 is an important oxide because of its catalytic, photocatalytic and electrochromic properties [15–17].

The various transformations were followed by X-ray diffraction, transmission electron microscopy and by ^{119}Sn and ^{57}Fe Mössbauer spectroscopy. The thermal stability of the polymorphs was studied by differential scanning calorimetry.

SSDI 0925-8388(95)01596-5

2. Experimental details

Continuous grinding was performed in a planetary ball mill (Fritsch Pulverisette 7) with a powder to ball weight ratio R of 1/40. The grinding tools are made either of (Fe-13% Cr) steel (vial ≈ 50 cm^3 and seven balls of diameter $\phi \sim 13$ mm) or of cubic yttria-stabilized zirconia (space group Fm3m, lattice parameter $a = 0.5103$ (1) nm) (vial ≈ 50 cm^3 and six balls of diameter $\phi \approx 13$ mm). The specific shock powers P injected during the ball-milling process have been obtained from powers calculated by Abdellaoui and Gaffet ([11,18] and personal communication). They are:

- $P = 2.7$ W/g/ball for steel tools and $R = 1/40$
- $P = 3.3$ W/g/ball and 1.7 W/g/ball for yttria-stabilized zirconia tools with $R = 1/40$ and 1/20 respectively

For $R = 1/40$, the specific powers are similar for steel and zirconia tools. The starting materials were: (1) SnO_2 (Labosi): tetragonal form, lattice parameters $a = 0.4737$ (2) nm, $c = 0.3184$ (2) nm as compared with $a = 0.4738$ nm, $c = 0.3189$ nm given by the Joint Committee on Powder Diffraction Standards (1969) (JCPDS, Card 21-1250)); (2) Y_2O_3 (Labosi): bixbyite form (space group Ia3), lattice parameter $a = 1.0604$ (2) nm, identical with the JCPDS value (Card 25-1200); (3) WO_3 (Merck): monoclinic form (space group $P2_1/c$), lattice parameters $a = 0.7678$ (7) nm, $b = 0.7516$ (7) nm, $c = 1.0529$ (7) nm, $\beta = 136.01$ (3)° compared with published parameters $a = 0.7692$ (1) nm, $b = 0.7540$ (1) nm, $c = 1.0527$ (2) nm, $\beta = 136.06$ (5)° [19].

The powders and balls were introduced in the vials and sealed in a glove box under an argon atmosphere. The powders were milled for different times varying from 30 min to 8 h. The resulting powders were all characterized by X-ray diffraction (XRD) using Co$K\alpha_1$ ($\lambda = 0.17889$ nm) radiation and by ^{119}Sn Mössbauer spectroscopy for SnO_2 samples. Some powders were further characterized by transmission electron microscopy (TEM). The TEM images, the electron diffraction patterns and the high-resolution electron microscopy (HREM) images were taken in a Philips CM200 electron microscope at 200 kV. Powder grains were placed between two glass plates and rubbed together. Samples suitable for TEM were collected by rubbing together one of the latter plates and a copper grid covered with amorphous carbon. Samples for TEM were also prepared by a second method: powder grains were dispersed in distilled water, ultrasonically processed and collected on a TEM grid 24 h later. Electron microdiffraction patterns (EDP) were obtained in nanoprobe mode with a probe of about 6.5 nm. X-ray microanalysis was performed with an EDAX DX-4 analyser. Room temperature ^{57}Fe Mössbauer spectra were recorded to characterize the contamination by steel after grinding. The thermal stabilities of the different phases were investigated by heating powders either in sealed glass tubes or under argon in SETARAM low (1073 K) or high (2000 K) temperature differential scanning calorimeters (DSC).

3. Results

3.1. TiO_2

Begin-Colin et al. [2] have used X-ray diffraction to show that the high-pressure modification TiO_2-II, with an α-PbO_2-type structure, forms transiently during room temperature grinding of anatase TiO_2. Further TEM observations (Fig. 1) unambiguously confirm the presence of the TiO_2-II phase in powders ground for 3 min. The X-ray diffraction patterns of the latter powders reveal a strong broadening ($\Delta 2\theta \sim 2°$) of the peaks associated with TiO_2-II [2], which is explained by nanometre-sized crystallites (Fig. 1). Nanometre-sized domains of rutile and of TiO_2-II coexist in the

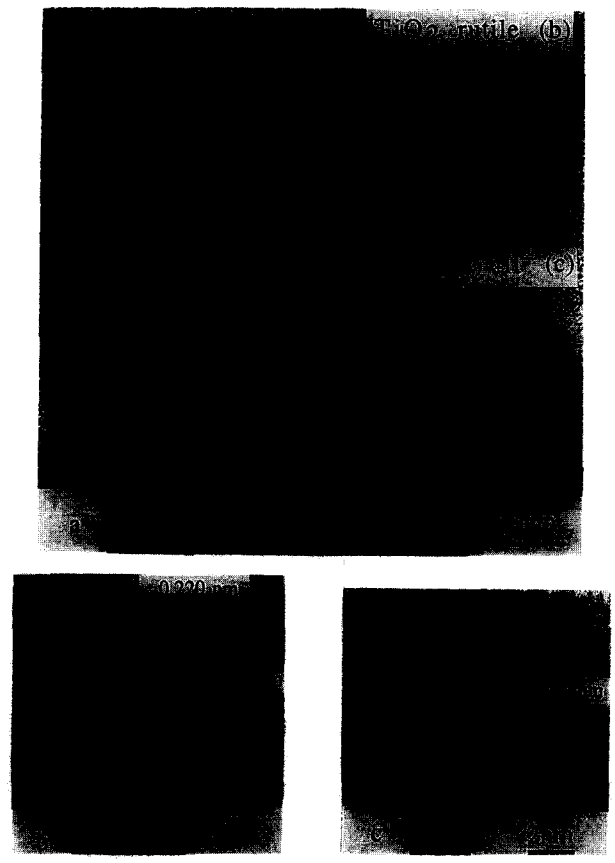

Fig. 1. (a) TEM micrograph of a particle of anatase TiO_2 ground for 3 min. Nanometre-sized domains of rutile and of TiO_2-II (such as (b) and (c)), with an average size of about 10–15 nm, coexist in the particle. Anatase is not observed. (b) [112] lattice image of rutile. (c) [101] lattice image of TiO_2-II.

studied particles. Only untransformed powder particles of anatase or transformed particles which do not contain anatase have been observed by TEM. This observation may not, however, be of statistical significance.

3.2. SnO_2

Grinding of cassiterite is worth being reported as it clearly reveals that redox reactions take place at the interfaces between powder and metallic tools. Cassiterite SnO_2 (tetragonal, space group P42/mnm) was milled for $t_g = 30$ min. and 4 h respectively with steel grinding tools. After milling, every ball was covered with a bright layer which was rich in tin. However, the XRD patterns of the powder exhibit no characteristic diffraction peaks of tin metal or of Fe–Sn intermetallic compounds. All the diffraction peaks can be indexed with reference to the cassiterite structure. ^{119}Sn Mössbauer spectroscopy shows, however, the existence of reduced tin in the form of Sn^{2+} in the ground powders (Fig. 2(b)). The quadrupole splitting is 1.90 ± 0.05 mm s^{-1} for the Sn^{2+} doublet, in very good agreement with the values reported for Sn^{2+} in various tin oxides (average value of 1.92 mm s^{-1}) by Neumann et al. [20]. Using the recoil-free factor ratio $f(SnO_2)/f(SnO) = 1.88 \pm 0.35$ given by Stjerna et al. [21], we calculate a mean composition $SnO_{1.74\pm0.04}$ for powders ground for 4 h. Avvakumov et al. [12] have studied the reduction of SnO_2 by milling in a planetary ball mill. They do not observe phase transformations. They suggest that a reduction of SnO_2 may have occurred on the walls of the vial and on the steel balls. Mössbauer spectroscopy is a better method than XRD for characterizing the pollution of the ground powders by steel. Two days were necessary to record a well resolved ^{57}Fe spectrum. The contamination level is therefore low. The Mössbauer spectrum for $t_g = 4$ h has been fitted with a sextuplet which is associated with iron in steel (proportion ~19%) and with two doublets related to Fe^{2+} and Fe^{3+} components which are present in equal proportions. The latter doublets indicate that metallic Fe reacts with SnO_2. The main reduction reaction occurs, however, at the interface between powder particles and balls. The bright layers which cover the steel balls after milling have been studied by ^{119}Sn Mössbauer spectroscopy. The spectra show the presence of metallic β-Sn and of Sn^{4+} and Sn^{2+} components which correspond to an average oxygen content $x \sim 1.7$ in SnO_x (Fig. 2(c)).

To avoid the reduction of SnO_2 by balls, milling has been performed with zirconia grinding tools. As in the previous experiment, phase transformations do not occur in ground powders. The balls remain, however, unaltered after milling. ^{119}Sn Mössbauer spectra (Fig. 2(a)) confirm that the ground powders only contain

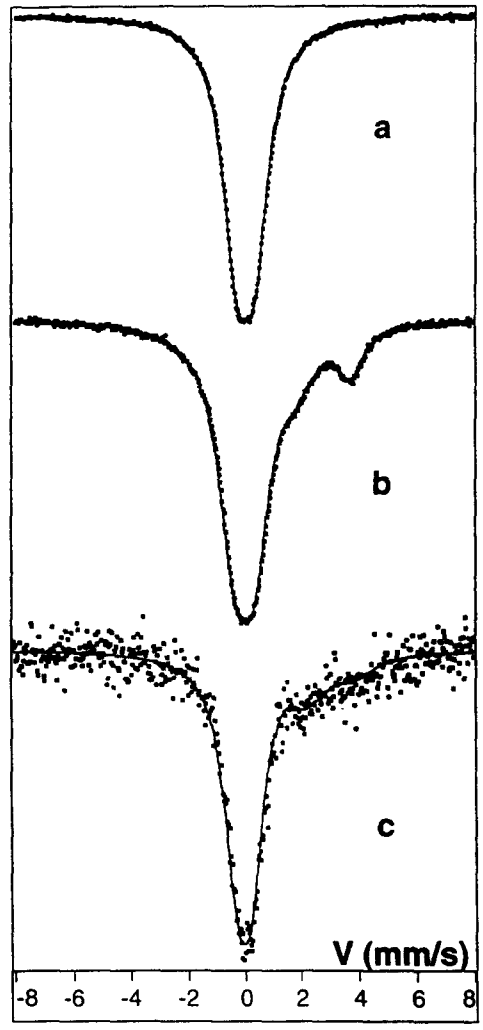

Fig. 2. ^{119}Sn room temperature Mössbauer spectra of (a) SnO_2 ground for 4 h in a zirconia vial with zirconia balls; (b) SnO_2 ground for 4 h with steel media; (c) layers covering steel balls after grinding SnO_2 in a steel vial for 4 h.

Sn^{4+}. The lattice parameters of SnO_2 calculated from the XRD patterns are: $a = 0.4736$ (5) nm, $c = 0.3180$ (4) nm and $a = 0.4737$ (4) nm, $c = 0.3182$ (4) nm when powders are ground with steel tools and with zirconia tools respectively. These values are almost identical with the lattice parameters of the starting tin oxide (Section 2).

3.3. Y_2O_3

Cubic Y_2O_3 (space group, Ia3) transforms into a monoclinic form when grinding is performed with steel vial and balls [5]. The monoclinic form is the major phase observed after 30 min and 2 h grinding. A small quantity of an amorphous phase is furthermore detected after 2 h grinding (Fig. 3). The amount of amorphous phase increases during prolonged grinding. Rühle and Steffens [6] have milled cubic Y_2O_3 for longer times (from 3 h to 110 h). They do not report

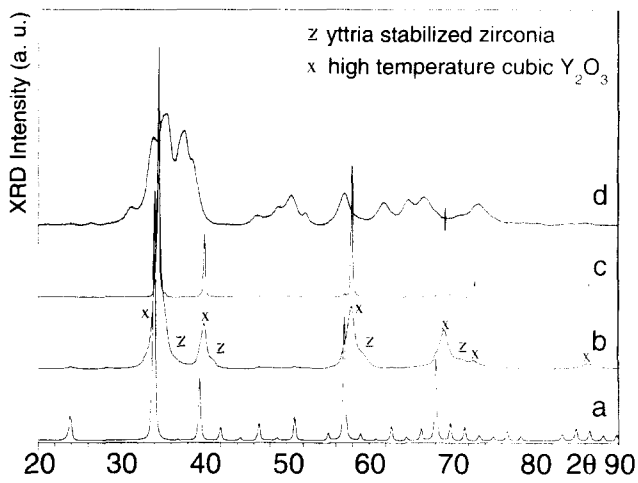

Fig. 3. XRD patterns (CoKα) of Y_2O_3: (a) starting oxide; (b) ground for 4 h in a zirconia vial with zirconia balls (x: high-temperature cubic form Y_2O_3, z: yttria stabilized zirconia); (c) ground for 4 h with zirconia tools and annealed at 1673 K for 1 h; (d) ground for 2 h with steel tools (all peaks different from those of the starting oxide correspond to the monoclinic form).

the formation of the monoclinic phase and only discuss amorphization. As the most intense diffraction lines of the cubic and monoclinic phases are rather close and are broadened by milling, it is indeed difficult to detect the monoclinic form in the presence of a significant amount of amorphous phase.

The lattice parameters of monoclinic Y_2O_3 (space group, C2/m) are: $a = 1.391$ nm, $b = 0.348$ nm, $c = 0.859$ nm, $\beta = 100.15°$ [22,23]. The lattice parameters are difficult to derive from our XRD patterns, as diffraction peaks are broad. We calculate nevertheless: $a = 1.38$ (± 0.005) nm, $b = 0.35$ (± 0.005) nm, $c = 0.86$ (± 0.005) nm, $\beta = 100.4°$ (4) in reasonable agreement with the published values. The thermal stability of the monoclinic phase has been thoroughly studied (Table 1). The monoclinic form obtained by grinding ($t_g = 6$ h) remains stable even after having been heated for two days at 923 K or after a heating–cooling cycle up to 1073 K at a rate of 10 K min^{-1}. A high-temperature DSC experiment shows the existence of an exothermic peak at ~1173 K upon heating (Fig. 4). It is associated with an irreversible monoclinic → cubic transformation

Table 1
Reported thermal stability of monoclinic Y_2O_3

Reference	Thermal stability of monoclinic Y_2O_3
[41]	In air at 1273 K for several hours
[22]	In air at 1173 K for several hours
[39]	A few hours at 1173 K
[23]	1 h at 1173 K 5 min. at 1273 K
[42]	Depends on grain size The transformation to cubic Y_2O_3 is complete at 1148 K

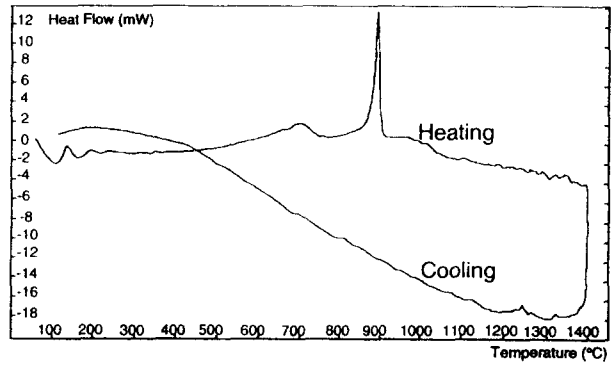

Fig. 4. DSC curves of Y_2O_3 milled for 6 h with steel tools.

and this temperature is of the same order of that of other authors (Table 1). After cooling down to room temperature, XRD patterns show the peaks associated with the cubic form. When milling is performed with steel tools that are not hard enough (Vickers hardness of 275 instead of 760 for the present grinding tools), diffraction peaks of a $YFeO_3$ compound are also observed.

When milling is performed in a zirconia vial with zirconia balls, a cubic modification of Y_2O_3, different from the original one, appears after 4 h milling. The initial cubic form is still present but in a smaller proportion than the new modification (Fig. 3). The space group (Fm3m) of the cubic polymorph that is formed by grinding can be deduced by isotopy with zirconia. The milled powders contain in addition a small amount of zirconia (space group Fm3m). Both phases have similar XRD patterns with very close diffraction lines. To reduce significantly the amount of zirconia, the powder to ball weight ratio was increased ($R = 1/20$), the cubic polymorph was formed and the milled powder was sifted. The XRD pattern of the sieved powder does not display the characteristic diffraction lines of zirconia. The lattice parameter of the cubic polymorph, before and after thermal treatment at 1673 K, is $a = 0.5232$ nm (Table 2). The electron diffraction pattern of a particle of Y_2O_3 is shown in Fig. 5. The Zr content was determined in situ by energy dispersive X-ray spectroscopy to be 0.5 at.%. Nanometre-sized domains with a mean diameter of about 15 nm are observed. As the most intense diffraction spots of the two cubic modifications of Y_2O_3 almost coincide, it is difficult to differentiate between them from EDP. The EDP of Figs. 5(b) and (c) are, however, attributed to the cubic structures with Fm3m and Ia3 space groups respectively. Katagiri et al. [24] have synthesized a new face-centred cubic modification of Y_2O_3 at 2493 K by a laser beam heating technique. The latter high-temperature form is considered to have a fluorite-type structure (Fm3m, Fig. 7(a), $a = 0.52644$ (3) nm) where one fourth of the

Table 2
Relative intensities and interplanar distances for the X-ray diffraction pattern of the cubic Fm3m modification of Y_2O_3 formed by grinding bixbyite type yttria (space group Ia3) with zirconia tools: $d_{observed}$ (d_{obs}) and $d_{calculated}$ (d_{calc}) correspond to the calculated interplanar distances assuming that the space group is Fm3m and $a = 0.5232$ nm

$h\,k\,l$	I_{obs}	d_{obs} (1) (nm)	d_{cal} (nm)
1 1 1	100	0.302	0.3021
2 0 0	23	0.261	0.2616
2 2 0	33	0.185	0.1850
3 1 1	21	0.158	0.1578
2 2 2	4	0.151	0.1511
4 0 0	3	0.131	0.1308
3 3 1	8	0.120	0.1201
4 2 0	3	0.117	0.1170
4 2 2	4	0.107	0.1068

oxygen sites are randomly vacant. Both the observed XRD line intensities and lattice parameters suggest that the high-temperature cubic modification and the ground cubic polymorph may represent the same phase. The cubic polymorph ground for 4 h is stable after being heated up to 1673 K at 10 K min^{-1}, maintained at that temperature for one hour and cooled down (Fig. 3).

3.4. WO_3

The XRD patterns of powders of monoclinic WO_3, the stable form of WO_3 between 290 K and 583 K, milled for different periods with steel vial and balls indicate that no phase transformations occur. Only a broadening of monoclinic WO_3 diffraction peaks is noticed (Fig. 6(b)). Mössbauer spectra show that contamination of WO_3 by Fe remains very low. A very small signal-to-noise ratio indicates indeed that the amount of iron lies at the lower detection limit of the technique. We have, however, observed that WO_3 reacts with steel when milling is performed with softer steel tools. The diffraction lines of $FeWO_4$ and WO_2 are indeed identified after 2 h of milling (Fig. 6(c)). The structure of WO_2 is monoclinic (space group $P2_1/c$) while $FeWO_4$ is Ferberite (space group P2/c, [25]). The presence of $FeWO_4$ is confirmed by Mössbauer spectroscopy.

Powders ground for 4 h with zirconia tools are composed of WO_3 oxide with a cubic structure of the ReO_3 type and zirconia (Fig. 6(d)). Clear differences exist between the XRD patterns of the cubic and of the monoclinic polymorphs (Fig. 6, Table 3). It is more difficult to discriminate between monoclinic WO_3 and cubic WO_3 with TEM, as interplanar distances deduced from lattice fringes are not precise enough (± 0.01 nm). Moreover, the EDP of Figs. 7(b) and (c) may be indexed with a cubic as well as a monoclinic structure. For monoclinic WO_3, supplementary diffraction spots, with weak to moderate intensities, should be observed but are not. HREM images show nanometre-sized domains, with an average size of about 20 nm (Fig. 7(a)). Zirconia in ground powders has the same lattice parameter as the original zirconia and is probably uncombined or at most slightly combined with WO_3. The lattice parameter of cubic WO_3 ($t_g = 4$ h) is $a = 0.377$ (1) nm. This compares favourably to published values: in thin films containing cubic WO_3, $a = 0.3838$ (2) nm and $a = 0.388$ nm have been measured respectively and calculated from ionic radii [26]. Moreover, a lattice parameter $a = 0.3714$ nm has been measured by Yamaguchi et al. [27] in cubic WO_3

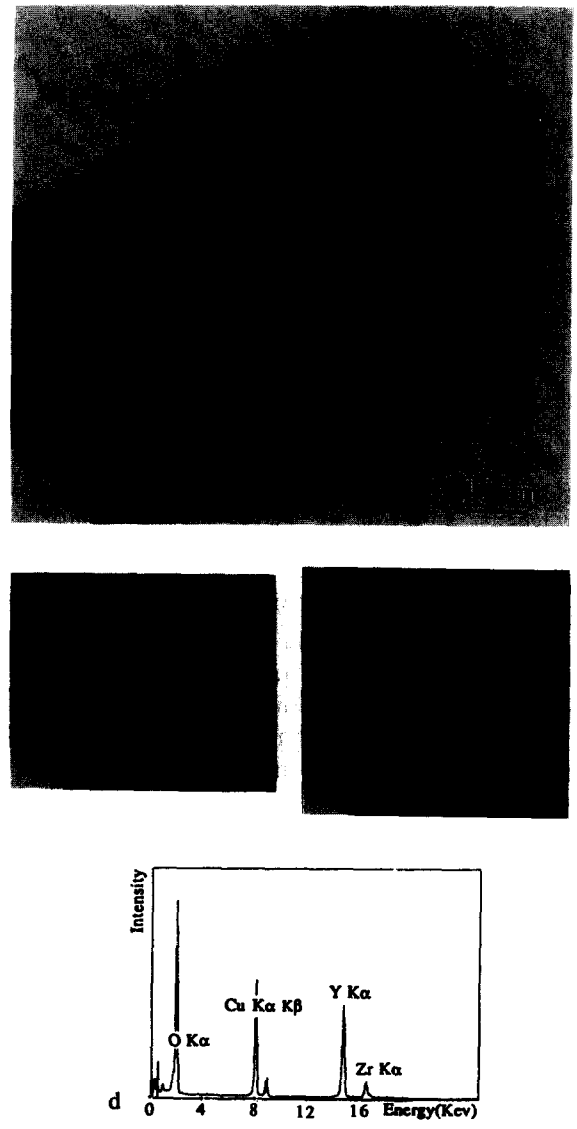

Fig. 5. (a) TEM micrograph of a particle of Y_2O_3 ground for 4 h with zirconia balls in a zirconia vial with domains with an average size of about 15 nm. Electron diffraction patterns of cubic Y_2O_3: (b) of zone axis [011] (space group Fm3m) and (c) of zone axis [011] (starting oxide, space group Ia3). (d) Energy dispersive X-ray spectrum for the particle shown in (a). The copper peaks originate from the sample holder and from the grid.

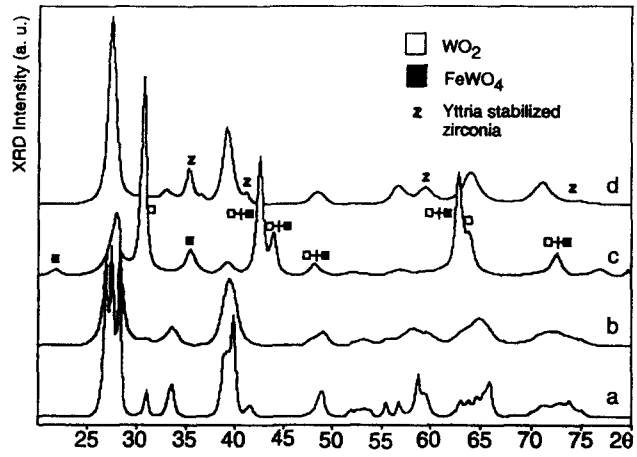

Fig. 6. XRD patterns (CoKα) of WO_3: (a) starting oxide; (b) ground for 4 h in a steel vial with steel balls; (c) ground for 4 h with ductile steel tools; (d) ground for 4 h in a zirconia vial with zirconia balls.

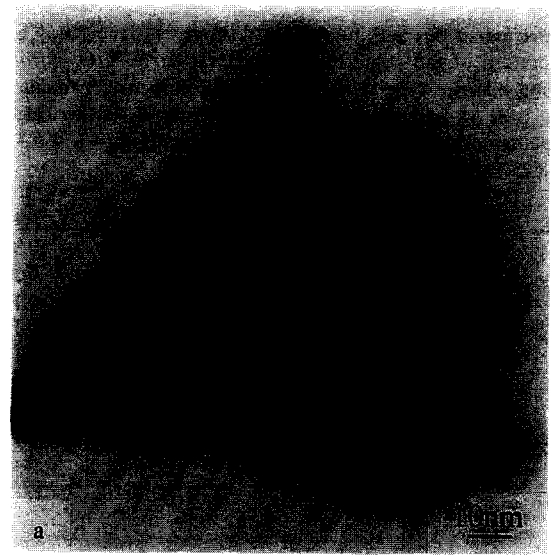

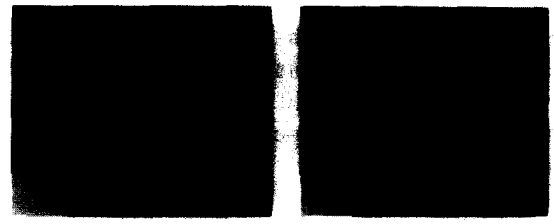

Fig. 7. (a) TEM micrograph of a particle of WO_3 ground for 4 h with zirconia balls in a zirconia vial showing domains with an average size of about 20 nm. Electron diffraction patterns of cubic WO_3: (b) of zone axis [011] and (c) of zone axis [021].

formed by dehydration of WO_3 H_2O. XRD results for the cubic modification are collected in Table 3. The XRD patterns (Fig. 6) of powders with zirconia tools exhibit narrower diffraction lines than those of powders ground with steel tools. The latter patterns appear simply as broadened XRD patterns of the starting powder. The full width at half maximum of the broad envelope at $\sim 27.5°$ (Fig. 6) is $\sim 0.9°$ and 1.8° in the case of powders ground for 4 h with zirconia tools and with steel tools respectively. The aforementioned results confirm that a phase transformation only takes place when grinding is performed with zirconia tools. The concentrations of inserted elements in tungsten bronzes are usually large (A_xWO_3 with $x \geq 0.07$ [34,40]). Although a small amount of inserted Zr^{4+} ions may help to stabilize the ReO_3-type structure, this contamination effect cannot explain solely the observed structural transformation. This suggests that phenomena occurring at the interfaces between powder particles and steel balls, for instance a slight reduction of WO_3 difficult to quantify in the ground materials, play an important role.

Cubic WO_3 synthesized by Yamaguchi et al. [27] transformed into the orthorhombic oxide in the temperature range from ~ 563 K to ~ 593 K. It is less stable than the cubic modification formed by grinding which remains untransformed after having been

Table 3
Interplanar distances and relative intensities for the X-ray diffraction patterns of cubic WO_3 with an ReO_3-type structure and of monoclinic WO_3

h k l	[26]		[27]		Present work		WO_3 monoclinic		
	d_{obs} (5) (nm)	Relative intensity (%)	d_{obs} (5) (nm)	Relative intensity (%)	d_{obs} (5) (nm)	Relative intensity (%)	h k l	d_{obs} (5) (nm)	Relative intensity (%)
1 0 0	0.3833	100	0.371	100	0.3767	100	2 0 −2	0.3840	98
1 1 0	0.2712	73	0.2631	65	0.2661	53	0 2 0	0.3769	95
1 1 1	0.2217	6	0.2144	5	0.2172	12	0 0 2	0.3690	100
2 0 0	0.1916	37	0.1856	20	0.1884	22	2 2 −2	0.2691	42
2 1 0	0.1716	59	0.1661	25	0.1687	37	2 0 0	0.2667	26
2 1 1	0.1567	33	0.1516	15	0.1537	26	2 0 −4	0.2625	22
2 2 0	0.1357	17			0.1333	6	0 2 2	0.2615	49
							2 2 0	0.2177	15
							2 2 −4	0.2154	16
							0 4 0	0.1885	11
							0 4 2	0.1674	11
							2 4 0	0.1539	5

heated for 2 days at 773 K. DSC experiments display a small exothermic peak around 1043 K. The XRD patterns of the DSC samples, heated up to 1073 K at a rate of 10 K min^{-1}, after cooling to room temperature exhibit only the diffraction peaks of the monoclinic oxide.

4. Discussion

Four types of force act during milling: impact, attrition, shear and compression [28]. As modelled by Le Brun et al. [29], most commercial planetary mills operate in a mode which involves mainly friction on the inner wall of the vial. Shear plays an important role in defects [30] and in phase transformations which are induced by grinding (see for instance, Refs. [1,31]), particularly in such mills. Moreover, local temperature increases may be significant in oxide particles crushed between balls or trapped between vial and balls. The combined actions of shear and increased temperature enhance atomic mobilities and facilitate phase transformations. Shear induces, for instance, sliding of Cl–Mg–Cl double layers, which is responsible for particle size reduction and for structural disordering induced by dry grinding in cubic or hexagonal $MgCl_2$ [32]. The phase transformations, which occur during grinding in the oxides investigated here, can be related to the ability to rearrange structural units (in general MO_6 octahedra) which are the building bricks of the various structures. Such units, in some cases slightly distorted, still exist in the transformed oxides. The starting phases are in general transformed into denser phases which are often high-temperature/high-pressure phases when formed in equilibrium conditions.

Grinding induces phase transformations in TiO_2 which consist of successive rearrangements of TiO_6 octahedra frameworks (Fig. 8): anatase → α-PbO_2-type TiO_2-II → rutile (an unidentified phase is moreover formed for milling times shorter than 15 min. [2]). Haines and Léger [33] have studied the pressure-induced phase transformations of TiO_2 up to 49 GPa at room temperature. Two phase transitions are observed: a first transition from anatase to TiO_2-II and a second transition to a monoclinic baddeleyite ZrO_2-type structure. Rutile is much less compressible than either anatase or TiO_2-II. The bulk modulus increases from 59 GPa for anatase to 98 GPa for TiO_2-II [33] and to 211 GPa for rutile. It is 522 GPa for the monoclinic structure. As discussed by Haines and Léger [33], such results can be understood from the arrangements of chains of edge-sharing TiO_6 octahedra from which all three structures are built (Fig. 8). The chains are straight in rutile with relatively short Ti–Ti distances. They zigzag in anatase and TiO_2-II

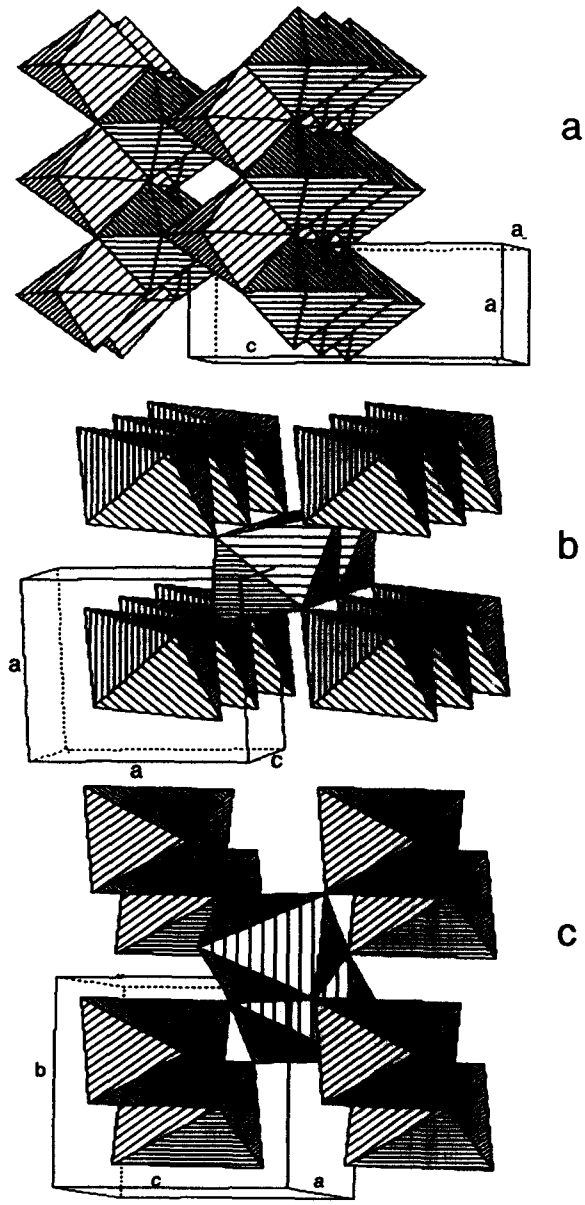

Fig. 8. Arrangements of octahedra in (a) anatase, (b) rutile and (c) TiO_2-II.

and may therefore be reorganized without resulting in too close an approach of Ti atoms. The shortest Ti–Ti distances are 0.296 nm and 0.310 nm and the mean first-neighbour distances are 0.345 nm and 0.343 nm for rutile and for TiO_2-II respectively [34]. Phase transformations induced by grinding or by applying high pressures will in general follow different routes. Cation jumps or slip on (001) planes of TiO_2-II are possible mechanisms, among others, for transforming TiO_2-II into rutile [34]. The monoclinic structure is not formed under our experimental conditions and the end-product is rutile, the stable form of TiO_2 at room temperature. The observation of nanometre-sized domains in completely transformed TiO_2 particles ground only for 3 min. (Fig. 1) suggests that domains

are formed immediately during a single collision event. Structural transformations may start simultaneously at many sites and propagate in a particle of anatase trapped between two balls or between vial and balls.

Cassiterite, which is isostructural to rutile, is partly reduced by grinding. The occurrence of redox reactions between powders and balls is clearly observed in that case. Monoclinic zirconia is similarly reduced when it is ground with steel tools [35]. This is further confirmed by the observation that Fe enters into nanocrystalline cubic zirconia generally as Fe^{2+} and only as Fe^{3+} when powder mixtures of zirconia and haematite Fe_2O_3 are ground with steel and zirconia tools respectively [35]. The material of the vials and balls also has a marked influence on the phase transformations which take place in the two oxides Y_2O_3 and WO_3. The observed effect cannot be ascribed to the small differences of injected specific powers between steel and zirconia tools (Section 2). The creation of defects in the ground oxide by reduction reactions with the metallic grinding tools combined with the action of shear may more easily induce structural transformations via, for instance, crystallographic shear [2,34,36]. The redox reaction produces in that case an effect which is in some way equivalent to the effect obtained by increasing the forcing parameter in systems driven away from thermal equilibrium by an external forcing such as irradiation [9]. In the absence of redox reactions, ground oxides will in general be converted into forms different from the previous ones. The nature of the atmosphere plays an important role on the nature of defects created by grinding and may thus have a strong influence on the observed transformations [30]. If the increase of the density of point defects due to reduction phenomena is combined with a reduced mobility, amorphization may be favoured in some ball-milled oxides as grains are moreover nanometre-sized. This may arise in oxides ground with metallic tools if structural unit rearrangements brought about by shear can no longer occur so easily in a structure already densified by previous phase transformations. Similar mechanisms have been recently proposed by Serghiou et al. [36] to account for pressure-induced amorphization and reduction of T-Nb_2O_5, but their model has not been confirmed in that particular case [37]. If the defect concentration is large enough, a defect-induced solid state amorphization may even take place [36,38]. This constitutes a tentative explanation for the full transformation in our experimental conditions of monoclinic Y_2O_3, which is $\approx 8\%$ denser than the starting bixbyite form [39], into amorphous Y_2O_3 by prolonged grinding with steel tools. In contrast, cubic Y_2O_3 is found without any amorphous phase when zirconia tools are used.

The bixbyite type structure of cubic Y_2O_3 is an ordered arrangement of three oxygen-deficient unit cells of a fluorite-type structure (Fig. 9 [40]). Two oxygen atoms, which lie on three body diagonals, are removed from a fluorite type unit cell to give the three building units of the bixbyite type structure shown in Figs. 9(c), (d) and (e). The XRD pattern of bixbyite type yttria is constituted of a superposition of diffraction lines from an average fluorite type structure and of superstructure lines which originate from the ordered arrangement of oxygen vacancies. Grinding thus induces a random distribution of c–d–e type cubes (Fig. 9). The superstructure diffraction lines thus disappear and the ground powder exhibits an XRD pattern of a fluorite-type structure identical with the high-temperature form of Y_2O_3 synthesized by Katagiri et al. [24] (Section 3.3).

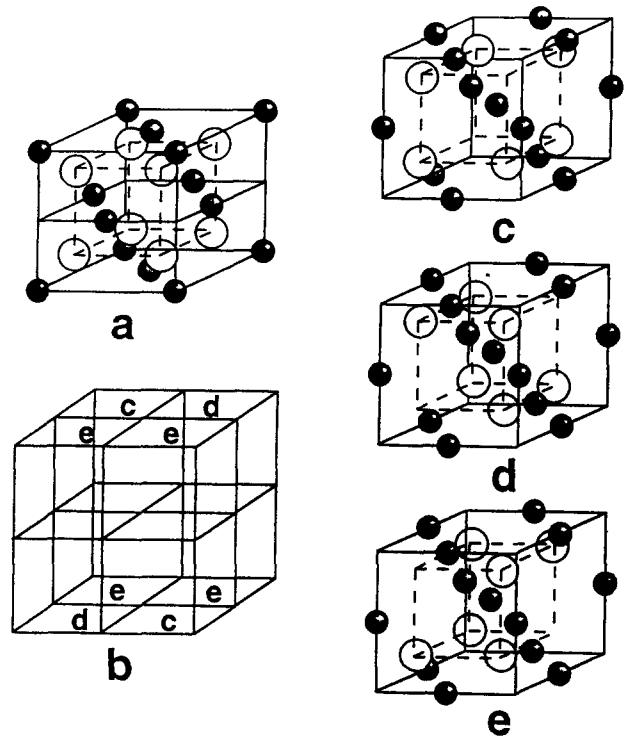

Fig. 9. Fluorite (a) and bixbyite (b) type structures of yttria; the bixbyite-type structure of yttria is an ordered arrangement of three oxygen deficient unit cells derived from the fluorite type structure as shown by c, d and e (inspired by Ref. [40]).

Monoclinic WO_3, a distorted ReO_3 type structure, transforms by grinding with zirconia tools into an ReO_3-type structure with regular octahedra sharing corners (Fig. 10 [34]).

5. Conclusion

Polymorphic transformations induced by dry ball milling in oxides depend sensitively on the nature of the materials constituting vials and balls as oxido-

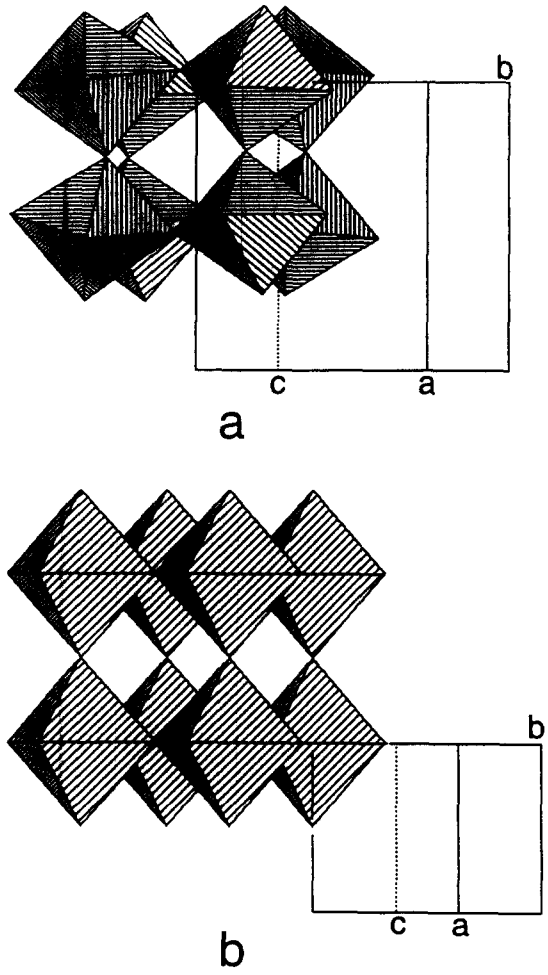

Fig. 10. Arrangements of octahedra in the monoclinic structure of WO_3 and in the ReO_3-type structure.

reduction reactions take place between metallic grinding tools and oxide particles. Possible structural mechanisms have been invoked to explain such differences. In the case of steel tools, redox reactions lead to the formation of mixed oxides containing iron, as shown by ^{57}Fe Mössbauer spectroscopy, which is a powerful technique for refined characterization of the unavoidable contamination by iron of all kinds of ground powders. In the case of SnO_2, steel balls are even covered with tin-rich bright layers after grinding for some hours. When ground with zirconia tools, cubic yttria is transformed into cubic yttria with a fluorite-type structure, while monoclinic tungsten oxide is transformed into a cubic oxide with a ReO_3 type structure. In contrast, a monoclinic modification of cubic yttria is formed when grinding is performed with steel tools. In all cases, nanometre-sized domains are observed with TEM and even after grinding times as short as a few minutes in the case of TiO_2. Finally, the way systems are driven far from the usual thermodynamical equilibrium [9–11] by mechanical actions may depend in some cases on physico-chemical conditions (atmosphere, chemical nature of grinding tools).

Acknowledgements

The authors are grateful to the European Economic Community for financial support (Science Program, contract no. CT91-0668) and to Mr P. Delcroix for help in Mössbauer spectroscopy. They also wish to thank Professor A. Mocellin (Ecole des Mines) and Professor P. Matteazzi (University of Udine, Italy) for useful discussions and Drs E. Gaffet and M. Abdellaoui (Institut Polytechnique de Sévenans) for useful information about injected powers.

References

[1] I.J. Lin and S. Nadiv, *Mater. Sci. Eng., 39* (1979) 193.
[2] S. Begin-Colin, G. Le Caër, A. Mocellin and M. Zandona, *Phil. Mag. Lett., 69* (1994) 1.
[3] I.J. Lin, S. Nadiv and P. Bar-On, *Thermochim. Acta, 148* (1989) 301.
[4] P.A. Zielinski, R. Schulz, S. Kaliaguine and A. Van Neste, *J. Mater. Res., 8* (1993) 2985.
[5] D. Michel, F. Faudot, E. Gaffet and L. Mazerolles, *Revue de Métallurgie, février* (1993) 219.
[6] M. Rühle and Th. Steffens, *Z. Metallkd., 83* (1992) 6.
[7] T. Ikeya and M. Senna, *J. Mater. Sci., 22* (1987) 2497.
[8] T. Ikeya and M. Senna, *J. Non-Cryst. Solids, 105* (1988) 243.
[9] G. Martin and P. Bellon, *Metall. Sci. Technol., 9* (1991) 61.
[10] Y. Chen, R. Le Hazif and G. Martin, *Solid State Phenom., 23&24* (1992) 271.
[11] M. Abdellaoui and E. Gaffet, *J. Alloys Comp., 209* (1994) 351.
[12] E.G. Avvakumov, V.E. Dyakov, A.I. Matytsin and A.M. Staver, *Akademiya Nauk SSSR, Sibirskoe Otdelenie-Fizika Goreniya i Vzryva, 6* (1975) 922.
[13] G. Le Caër, R. de Araujo Pontès, D. Osso, S. Begin-Colin and P. Matteazzi, *36èmeColloque de Métallurgie* , INSTN, Saclay, June 22–23 1993, *J. de Phys. IV, 4* (1994) 233.
[14] J.S. Benjamin, *Metall. Trans., 1* (1970) 2943.
[15] M. Ashokkumar and P. Maruthamuthu, *J. Photochem. Photobiol., A: Chemistry, 49* (1989) 249.
[16] S.I. Cordoba de Torresi, A. Gorenstein, R.M. Torresi and M.V. Vazquez, *J. Electroanal. Chem., 318* (1991) 131.
[17] Y.R. Do, W. Lee, K. Dwight and A. Wold, *J. Solid State Chem., 108* (1994) 198.
[18] M. Abdellaoui and E. Gaffet, *Acta Metall.*, in press.
[19] B.O. Loopstra and H.M. Rietveld, *Acta Cryst. B, 25* (1969) 1420.
[20] H.G. Neumann, P. Zeggel and K. Melzer, *J. Non-Cryst. Solids, 108* (1989) 128.
[21] B. Stjerna, C.G. Granqvist, A. Seidel and L. Häggström, *J. Appl. Phys., 68* (1990) 6241.
[22] H.R. Hoekstra, *Inorg. Chem., 5* (1966) 754.
[23] V. Gourlaouen, G. Schnedecker, A.M. Lejus, M. Boncoeur and R. Collonges, *Mater. Res. Bull., 28* (1993) 415.
[24] S. Katagiri, N. Ishizawa and F. Marumo, *Powder Diff., 8* (1993) 60.
[25] D. Ülkü, *Z. Kristallogr., 124* (1967) 192.
[26] L.S. Palatnik, O.A. Obol'yaninova, M.N. Naboka and N.T.

Gladkikh, *Izvestiya Akademii Nauk SSSR, Neorg. Mat., 9* (1973) 801.
[27] O. Yamaguchi, D. Tomihisa, H. Kawabata and K. Shimizu, *J. Am. Ceram. Soc., 70* (1987) C-94.
[28] *Materials Handbook*, 9th edn, Powder Metallurgy, American Society for Metals, Ohio, 1988.
[29] P. Le Brun, L. Froyen and L. Delaey, *Mater. Sci. Eng. A, 161* (1993) 75.
[30] U. Steinike, U. Kretzschmar, I. Ebert, H.P. Hennig, L.I. Barsova and T.K. Jurik, *Reactivity of Solids, 4* (1987) 1.
[31] V.V. Boldyrev, *J. Chim.-Phys., 83* (1986) 821.
[32] J.C.J. Bart, *J. Mater. Sci., 28* (1993) 278.
[33] J. Haines and J.M. Léger, *Physica B, 192* (1993) 233.
[34] B.G. Hyde and S. Andersson, *Inorganic Crystal Structures*, Wiley, New York, 1989.
[35] F. Wolf, G. Le Caër, S. Bégin-Colin, and G. Braichotte, *Proc. First Int. Conf. Mechanochemistry*, Kosice, 23–26 March 1993, Cambridge Interscience, in press.
[36] G.C. Serghiou, R.R. Winters and W.S. Hammack, *Phys. Rev. Lett., 68* (1992) 3311.
[37] J.S. Tse, D.D. Klug and Z.H. Lu, *Phys. Rev. B, 49* (1994) 9180.
[38] H.J. Fecht, *Nature, 356* (1992) 133.
[39] R. McPherson, *J. Mater. Sci., 18* (1983) 1341.
[40] F.S. Galasso, *Structure and Properties of Inorganic Solids*, Pergamon Press, Oxford, 1970.
[41] H.R. Hoekstra and K.A. Gingerich, *Science, 145* (1964) 1163.
[42] H. Hahn, *Nanostructured Mater., 2* (1993) 251.